Identification of Critical Operating Boundaries and Recommended Actions for Power Systems Subject to Constrained Perturbations

Brian Johnson
Department of Mathematics
Case Western Reserve University
Cleveland, Ohio, USA
Email: brian.c.johnson@case.edu

Tomás Tinoco De Rubira
Grid Operations and Planning
Electric Power Research Institute
Palo Alto, California, USA
Email: ttinoco@epri.com

Adam Wigington
Grid Operations and Planning
Electric Power Research Institute
Palo Alto, California, USA
Email: awigington@epri.com

***Abstract*—Identifying critical operating boundaries as well as systems changes for mitigating violations and increasing security margins are key for the secure and reliable operation of power systems. However, these tasks are computationally intensive and hence their use in practice is difficult and limited. Previous works have explored computationally efficiency techniques for performing these tasks, but key problem aspects have not yet been properly considered, such as the fact that some information is often known about the possible perturbations that could affect the system, such as bounds. In this work, techniques are proposed for extending previous works based on linearized system models and matrix-free methods to consider constrained perturbations when estimating operating boundary distances and identifying suitable system changes.**

I. Introduction

Power systems have numerous security constraints that need to be considered, such as voltage stability constraints, branch thermal overload limits, bus voltage magnitude limits, and dynamic stability constraints, in order to ensure a secure and reliable operation. Traditionally, security assessment practices for identifying potential operational issues and corresponding mitigating actions have typically relied on operator experience and on offline studies performed hours or days in advance due to their high computational cost. However, power systems are now being operated closer to their limits and are subject to more severe and unpredictable changes due to factors such as deregulation, demand response, and variable and distributed generation. Hence, there is a need for improving security assessment tools to better support system operators and planners in this more challenging environment. In particular, improvements are needed for quickly and automatically identifying potential security issues and recommended system changes, and for communicating this information in a concise and intuitive manner [1].

Several research efforts have focused on developing new techniques for performing security assessment and determining suitable system changes. In particular, efforts have been made for developing techniques for representing security boundaries and for determining their proximity to the current operating point. In [2] and [3], various security constraints are considered and approaches for approximating boundaries using hyperplanes in the space of pre-selected critical quantities are described. The construction of the hyperplanes is done offline by stressing the critical quantities in different directions and performing system simulations. An alternative approach is described in [4] and [5], in which a neural network that is trained offline using simulations is used for mapping values of pre-selected critical quantities to system security measures. An approach for determining bounds on thermal security margins is described in [6]. The approach uses a linear system model based on sensitivities and expresses security margins in terms of changes in generator and load powers. A similar approach based on a linear model but using matrix-free techniques is considered in [1] and [7]. The approach is shown to be computationally efficient and able to identify potential critical thermal and voltage boundaries as well as recommended system directions in a matter of seconds even for large-scale systems, but it has important limitations. In particular, proximity to each boundary is measured based on the size, in the Euclidean norm sense, of the smallest generator and load perturbations needed to push the system to the boundary. This notion of proximity is too obscure for practice. Furthermore, the boundary proximity measure does not consider constraints on the possible system perturbations, and hence boundaries that are near but hard to reach due to these constraints may be incorrectly determined to be critical. Also, only recommended system directions are provided instead of concrete recommended actions. Lastly, the approach works under the assumption that the current operating point is secure, *i.e.*, it is not currently violating any of the considered security boundaries.

In this work, the limitations of the linear-model and matrix-free based approach considered in [1] and [7] are addressed while still preserving its promising computational efficiency and scalability. In particular, the approach is modified to measure boundary proximity in terms of the smallest total MVA system perturbations needed to push the system to the boundary, and to consider constraints on the possible system perturbations. Furthermore, the approach is extended to

provide concrete recommended actions that account for control adjustment limits, and to work with systems that are insecure at the current operating point.

This paper is organized as follows: In Section II, a mathematical description of the problem is provided. In Section III, the proposed methodology for modeling the system, identifying critical boundaries, and computing recommended actions is described. In Section IV, implementation details are discussed. In Section V, the results of numerical experiments are presented. Lastly, in Section VI, the work is summarized and next research steps are provided.

II. Problem Description

The problem considered consists of determining the most critical operating boundaries of a power system at a given operating point as well as any recommended system changes for mitigating security violations and increasing security margins.

The system is represented by the constraint $f(x, y) = 0$, where y are independent variables such as active powers of non-slack generators, active powers of loads, and susceptances of switched shunt devices, while x are dependent variables such as bus voltage magnitudes and angles, reactive powers of voltage-regulating generators, active powers of slack generators, and reactive powers of loads. This constraint enforces bus active and reactive power balance, bus voltage regulation by generators, and constant load power factors. It determines implicitly how the dependent variables x change when y changes. The independent variables represent quantities that have uncertainty associated with them, or controls that can be adjusted. The only information known about them is their current value, denoted by y_0, and bounds $y^{\min} \leq y_0 \leq y^{\max}$. The system has security constraints given by $h(x) \geq 0$, which include branch thermal limits, bus voltage magnitude limits, active power limits of slack generators, and reactive power limits of voltage-regulating generators. The goal is to determine the nearest individual boundaries $h_i(x) = 0$ and their proximity. The proximity of a boundary is defined as the smallest change in y needed to make $h_i(x) = 0$ hold. In particular, for boundary i, its distance from the current operating point is defined as $\text{sign}(h_i(x_0))\gamma^*$, where x_0 denotes the system state associated with y_0, and γ^* is the optimal objective value of

$$\begin{aligned} \underset{x,z}{\text{minimize}} \quad & \|z\|_1 \\ \text{subject to} \quad & h_i(x) = 0 \\ & f(x, y_0 + \bar{P}z) = 0 \\ & y^{\min} \leq y_0 + \bar{P}z \leq y^{\max}, \end{aligned} \tag{1}$$

where $\bar{P}$ is defined such that $z = \bar{P}^T y$ is the subvector of y that has only the potential system perturbation and not any controllable quantities. Hence, distances to boundaries not currently violated are positive, and to those currently violated are negative. Critical boundaries are those with the smallest signed distance. By convention, the optimal value of (1) is ∞ if infeasible, which corresponds to the boundary being unreachable. The ℓ_1 norm in (1) measures total system changes and better reflects notions of size of system perturbations used in practice than the Euclidean norm used in [1] and [7].

Recommended actions are defined as changes in y such as they maximize a specific security metric. In particular, the ideal recommended actions are defined as the optimal point of the following optimization problem:

$$\begin{aligned} \underset{x,z}{\text{maximize}} \quad & \mu \sum_i \log\big(\max\{\, h_i(x),\, \epsilon \,\}\big) \\ \text{subject to} \quad & f(x, y_0 + \tilde{P}z) = 0 \\ & y^{\min} \leq y_0 + \tilde{P}z \leq y^{\max}, \end{aligned} \tag{2}$$

where $\mu > 0$, $\epsilon > 0$, and $\tilde{P}$ is defined such that $z = \tilde{P}^T y$ is the subvector of y that has only controllable quantities and not any uncontrollable potential system perturbations. Since $f(x_0, y_0) = 0$ by definition and $y^{\min} \leq y_0 \leq y^{\max}$ by assumption, problem (2) is always feasible.

Problems (1) and (2) are nonlinear, non-convex, and potentially large-scale optimization problems. Moreover, the total number of security boundaries of a system, and hence the number of problem (1) instances to be solved, is very large, *e.g.*, in the hundreds of thousands, for large-scale systems. Therefore, solving these problems is not practical for performing security assessments and determining recommended actions fast. Speed is critical for times during which a system changes rapidly, and for being able to consider a large number of operating scenarios, *e.g.*, contingencies.

III. Methodology

In this section, the modeling methodology and computational techniques considered for trying to solve the problem described above are provided.

A. Model

The modeling approach considered is the same as that used and evaluated in [1] and [7] in order to allow for fast computations. More specifically, the constraint $f(x, y) = 0$ is linearized to obtain $Ax = b + Yy$, where A and Y are sparse matrices. Similarly, the security constraint $h(x) \geq 0$ is linearized to obtain $Cx \geq d$, where C is a sparse matrix. By exploiting the fact that A is invertible, except possibly at voltage stability limits, which are outside the scope of this work, the dependent variables can be eliminated, and the security constraints can be expressed purely in terms of y as $Qy \geq t$, where $Q := CA^{-1}Y$ is a potentially large and dense matrix, and $t := d - CA^{-1}b$. This transformation allows for efficient computations but care must be taken to avoid constructing the entire matrix Q.

B. Critical Boundaries

With the modeling approach described above, the problem of identifying nearest boundaries consists of solving

$$\begin{aligned} \underset{z}{\text{minimize}} \quad & \|z\|_1 \\ \text{subject to} \quad & q_i^T(y_0 + \bar{P}z) = t_i \\ & y^{\min} \leq y_0 + \bar{P}z \leq y^{\max} \end{aligned} \tag{3}$$

for each boundary i, where q_i is the i-th row of Q. Although problem (3) is much simpler than (1), it requires constructing q_i for each boundary, which is too slow if done for all boundaries of a large-scale system.

The approach considered here consists of a two-stage process. The first stage consists of an initial filter that considers all boundaries, say m_0, and selects a subset of $m_I \ll m_0$ intermediate boundaries that are highly likely to contain the $m_C \leq m_I$ nearest or most critical ones. For this first-stage filter, the proxy used for ranking boundaries utilizes the optimal objective value of

$$\begin{aligned} \underset{z}{\text{minimize}} \quad & \|z\|_2 \\ \text{subject to} \quad & q_i^T(y_0 + \bar{P}z) = t_i \end{aligned} \tag{4}$$

for each boundary i. The key here is that the optimal objective values of these problems can be estimated efficiently, accurately, and simultaneously using only matrix-vector products with the linear operator $Q\bar{P}$. Details about this process can be found in [1] and [7]. For the top m_I boundaries identified with this process, q_i can be constructed by performing two matrix-vector multiplications and a single linear solve with A^T, which needs to be factorized only once, and then problem (3) can be solved. To solve this problem fast, the custom procedure outlined in Procedure 1 is considered, where $|\cdot|$ denotes element-wise absolute value.

Procedure 1 Custom solver for (3)

Input: $y_0, y^{\min}, y^{\max}, \bar{P}, t_i, q_i \neq 0$
Output: Optimal objective value of (3)

$z \leftarrow 0,\ r \leftarrow t_i - q_i^T y_0,\ w \leftarrow \bar{P}^T q_i$
$u \leftarrow \bar{P}^T(y^{\max} - y_0),\ l \leftarrow \bar{P}^T(y^{\min} - y_0)$
for all $j \in \text{argsort}(-|w|)$ **do**
  if $w^T z - r = 0$ **then**
    return $\|z\|_1$
  else if $w_j = 0$ **then**
    return ∞
  end if
  $z_j \leftarrow z_j + \max\{\min\{(r - w^T z)/w_j, u_j - z_j\}, l_j - z_j\}$
end for
return ∞

In Section V, experimental results showing suitable values of m_I as percentages of m_0 for various power systems are presented as well as the performance of Procedure 1.

C. Recommended Actions

With the modeling approach described above, the problem of identifying recommended actions consists of solving

$$\begin{aligned} \underset{z}{\text{maximize}} \quad & \mu \sum_i \log\left(\max\{\, q_i^T(y_0 + \tilde{P}z) - t_i,\, \epsilon\,\}\right) \\ \text{subject to} \quad & y^{\min} \leq y_0 + \tilde{P}z \leq y^{\max}. \end{aligned} \tag{5}$$

The procedure proposed here for approximately solving this problem consists of the shifted-barrier matrix-free projected gradient ascent algorithm outlined in Procedure 2, which works with a sequence of subproblems with objective functions of the form $\mu \sum_i \log\left(q_i^T(y_0 + \tilde{P}z) - t_i + \eta\right)$ with suitable $\eta > 0$.

Procedure 2 Custom solver for (5)

Input: $y_0, y^{\min}, y^{\max}, \tilde{P}, t, Q, \epsilon > 0, \mu > 0, K > 0, M > 0$
Output: Approximate optimal point for (5)

$z \leftarrow 0$
$u \leftarrow \tilde{P}^T(y^{\max} - y_0),\ l \leftarrow \tilde{P}^T(y^{\min} - y_0)$
for all $k \in \{1, \ldots, K\}$ **do**
  $\eta = \max\left\{\max_i \left(\epsilon - Q(y_0 + \tilde{P}z) + t\right)_i, 0\right\}$
  for all $m \in \{1, \ldots, M\}$ **do**
    $r \leftarrow \left(Q(y_0 + \tilde{P}z) - t + \eta\right)^{-1}$
    $p \leftarrow \max\left\{\min\{z + \mu\tilde{P}^T Q^T r/m, u\}, l\right\} - z$
    $\alpha \leftarrow 1$
    while $\exists i, \left(Q(y_0 + \tilde{P}(z + \alpha p)) - t + \eta\right)_i \leq 0$ **do**
      $\alpha \leftarrow \alpha/2$
    end while
    $z \leftarrow z + \alpha p$
  end for
end for
return z

In Procedure 2, $(\cdot)^{-1}, \max\{\cdot,\cdot\}, \min\{\cdot,\cdot\}$ with vector arguments denote element-wise operations. The number of outer and inner iterations K and M, respectively, are kept fixed in order to have precise control of the computational requirements of the algorithm.

IV. Implementation

The techniques described in this work were implemented using the Python programming language. More specifically, the library `PFNET` [8] was used for constructing power networks and obtaining the matrices and vectors necessary to build the model described in Section III-A. The libraries `GRIDOPT` and `OPTALG` were used for computing operating points. Lastly, the scientific computing libraries `Scipy` and `Numpy` were used for implementing the algorithms described in Sections III-B and III-C. These routines have been integrated into the research-grade software `COB`, which is developed at the Electric Power Research Institute, in order to evaluate their usefulness in practice [9].

V. Numerical Experiments

In this section, numerical experiments that motivate and evaluate the performance of the techniques described in Section III are presented.

For the experiments, three power networks were considered. One was obtained from an electric utility in North America while the other two consist of synthetic cases developed by the research effort described in [10]. For all these cases, security constraints were taken to be bus voltage magnitude limits and any available branch thermal limits. For system perturbations, changes in all generator and load active powers were considered. For generators, bounds on active power changes were taken from the power flow files. For loads, bounds on

active powers were defined using $\pm 50\%$ of the demand data available in the power flow file. For possible control actions, the same generator and load active powers were considered together with changes in susceptance of switched shunt devices within the limits defined in the power flow files. Information about these cases including name, number of buses, number of security boundaries, number of system perturbations, and number of possible control actions is provided in Table I.

TABLE I
TEST CASES

name	buses	boundaries	perturbations	actions
Case A	2500	17656	1198	1335
Case B	10000	73028	6562	6947
Case C	25000	170956	11921	12768

The first experiment compared boundary distances with and without considering perturbation constraints, *i.e.*, $y^{\min} \leq y \leq y^{\max}$. The distances are referred to as "limit-aware" and "direct", respectively. The results obtained for Case A are shown in Figure 1. As the figure shows, these distances are not well correlated and hence using purely "direct" distances for ranking security boundaries, as considered in [1] and [7], can lead to misleading notions of proximity.

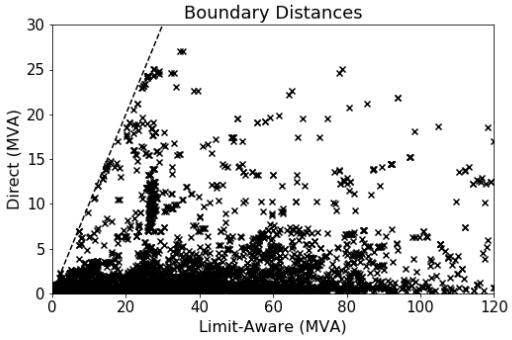

Fig. 1. Direct vs Limit-Aware Boundary Distances

The second experiment compared the speed of the custom Procedure 1 for solving (3) against that of the linear programming solver `clp` [1] and the conic solver `ecos` [11]. Figure 2 shows the average time spent by each solver computing the distance to each boundary for each test case (on a laptop with Ubuntu, 8 GM of RAM, and 2.8 GHz). As the figure shows, the custom procedure is about an order of magnitude faster than the standard solvers.

The third experiment evaluated the ability of the proposed two-stage procedure described in Section III-B to identify the most critical boundaries (for the linear model) using various numbers of intermediate boundaries m_I expressed as percentages of the total number of boundaries m_0. The results obtained are shown in Figures 3-5, where the ranking score is a normalized measure of the number of boundaries within each top k considered that are ranked in the correct

[1]projects.coin-or.org/Clp

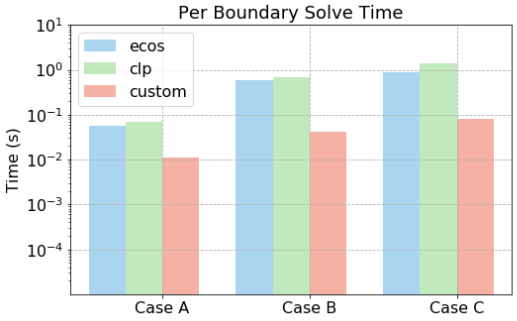

Fig. 2. Computation of Limit-Aware Boundary Distances

place with respect to the brute-force approach that solves (3) for all boundaries. As the figures show, using a number of intermediate boundaries m_I equal to only about 2% of m_0 appears to be enough to identify the 30-40 most critical boundaries of the cases considered. This means that only about 2% of the rows of Q need to be constructed and an equal number of instances of problem (3) need to be solved in order to identify up to $30-40$ of the most critical boundaries reliably, which represents significant computational savings.

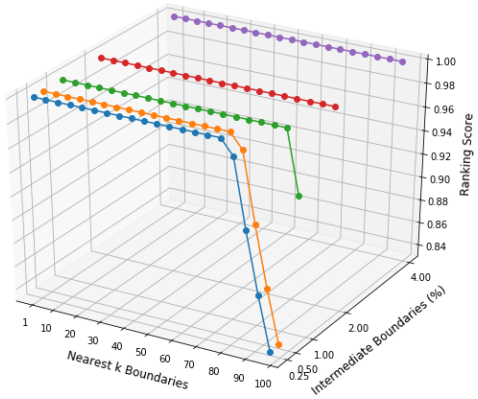

Fig. 3. Case A: Identification of Critical Boundaries

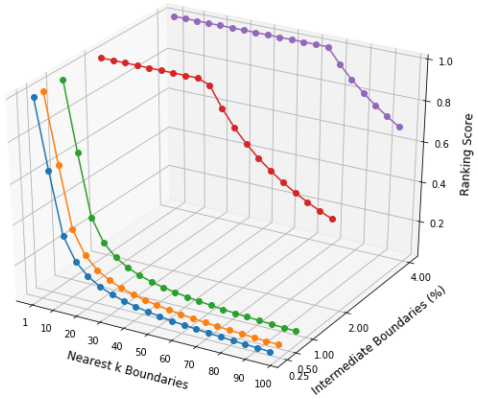

Fig. 4. Case B: Identification of Critical Boundaries

Lastly, the proposed algorithm for computing recommended actions was executed on each of the test cases. The parameters

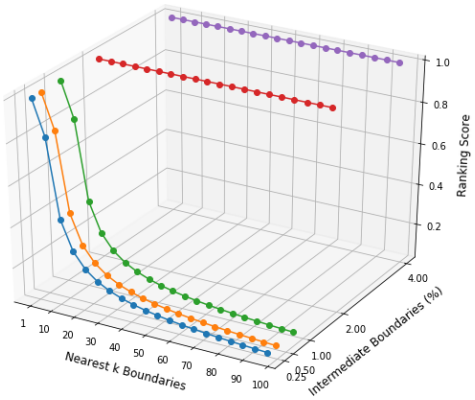

Fig. 5. Case C: Identification of Critical Boundaries

used were $\mu = 10^{-3}$, $\epsilon = 10^{-5}$, $K = 10$, and $M = 80$. The recommended actions obtained are shown in Figures 6-8 together with the critical boundaries using $m_I = 2.5m_0/100$ on visualization planes constructed using the techniques described in [1] and [7]. On the figures, the recommended actions are represented by an arrow, the green, red, blue, and yellow regions represent regions with no violations, thermal violations, voltage violations, and generator resource violations, respectively, and the dotted lines represent bounds on the controllable system changes. Performing these analyses took 4, 26, and 102 seconds for Case A, B, and C, respectively.

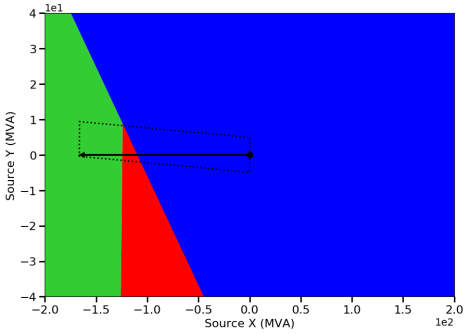

Fig. 6. Case A: Recommended Actions

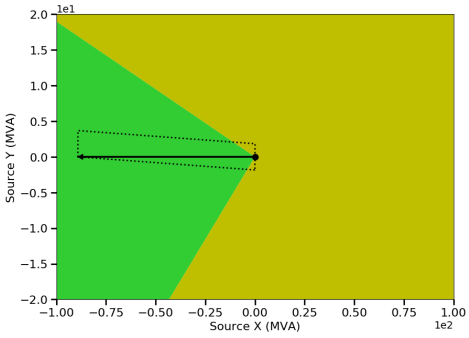

Fig. 7. Case B: Recommended Actions

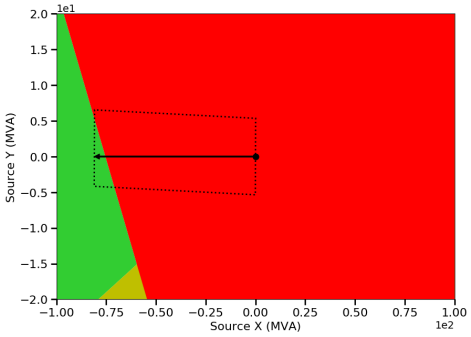

Fig. 8. Case C: Recommended Actions

VI. Conclusions

In this work, computational techniques have been described for identifying potential critical operating boundaries and recommended system changes for power systems subject to constrained perturbations. These techniques were based on a two-stage filtering procedure that leveraged a custom linear programming solver for computing boundary distances, and on a shifted-barrier matrix-free projected gradient ascent algorithm for computing recommended actions. These techniques have been tested on mid- and large-scale cases, and the results demonstrate their benefits.

Potential next research steps related to this work are the consideration of limits on the number of allowed recommended actions, and on correlations between the possible system perturbations.

References

[1] T. Tinoco De Rubira, "Numerical optimization and modeling techniques for power system operations and planning," PhD Thesis, Stanford University, March 2015.

[2] Y. Makarov, S. Lu, X. Guo, J. Gronquist, P. Du, T. Nguyen, and J. Burns, "Wide area security region," Pacific Northwest National Laboratory, Report PNNL-19331, Tech. Rep., 2010.

[3] T. Jiang, H. Jia, Y. Jiang, and J. Zhao, "Cutset-angle based wide area thermal security region and its application in China southern power grid," *International Transactions on Electrical Energy Systems*, 2014.

[4] J. McCalley, S. Wang, Q. Zhao, G. Z., R. Treinen, and A. Papalexopoulos, "Security boundary visualization for systems operation," *IEEE Transactions on Power Systems*, vol. 12, no. 2, May 1997.

[5] G. Zhou and J. McCalley, "Composite security boundary visualization," *IEEE Transactions on Power Systems*, vol. 14, no. 2, pp. 725–731, May 1999.

[6] F. Capitanescu and T. Van Cutsem, "Evaluating bounds on voltage and thermal security margins under power transfer uncertainty," in *Power Systems Computation Conference*, June 2002.

[7] R. Entriken, W. Murray, and T. Tinoco De Rubira, "Linear analysis for determining and visualizing critical thermal boundaries of power systems," in *IEEE Innovative Smart Grid Technologies Conference*, February 2015, pp. 1–5.

[8] M. Baltzinger, T. Tinoco De Rubira, and A. Wigington, "A modular and efficient modeling library for power flow network steady-state analysis and optimization," in *IEEE General Meeting*, August 2018.

[9] EPRI, *Critical Operating Boundaries (COB)*, Version 2.0, 3002013702, September 2018.

[10] A. Birchfield, T. Xu, K. Gegner, K. Shetye, and T. Overbye, "Grid structural characteristics as validation criteria for synthetic networks," *IEEE Transactions on Power Systems*, vol. 32, no. 4, pp. 3258–3265, July 2017.

[11] A. Domahidi, E. Chu, and S. Boyd, "ECOS: An SOCP solver for embedded systems," in *European Control Conference*, 2013, pp. 3071–3076.